The College of Engineering
University of Wisconsin-Madison

Wisconsin Electric Machines and Power Electronics Consortium

RESEARCH REPORT
90-24

A Five Phase Reluctance Motor With High Specific Torque

Hamid A. Toliyat, Longya Xu, Thomas A. Lipo
Dept. of Elec. and Comp. Eng.
University of Wisconsin-Madison
1415 Johnson Drive
Madison, WI 53706-1691

WEMPEC

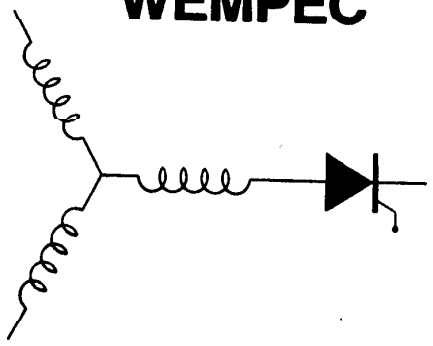

Department of Electrical and Computer Engineering
1415 Johnson Drive
Madison, Wisconsin 53706

A Five Phase Reluctance Motor with High Specific Torque

Hamid A. Toliyat
Student Member, IEEE

Longya Xu
Student Member, IEEE
University of Wisconsin-Madison
1415 Johnson Drive
Madison, WI 53705

Thomas A. Lipo
Fellow, IEEE

Abstract

An alternative topology for a synchronous reluctance motor (SRM) is proposed utilizing a novel five phase, concentrated winding, wye connected stator. The corresponding inverter requires only 10 transistors, each of which operate at a better switch utilization factor as a conventional three phase, six transistor bridge. It is shown that this machine is capable of producing about 12% more torque per RMS current than the normal 3 phase SRM.

Introduction

As the workhorse of industry, the prominence of the induction motor remains secure. Recently, however, improved types of permanent magnet and reluctance motors have prompted a revival of interest in such machines. In particular, the so-called switched reluctance [1] or variable reluctance motor [2], has attracted much attention. This type of machine is a doubly salient structure having projecting poles on both the stator and the rotor. By winding and sequentially exciting coils around the stator poles, reluctance torque is produced between adjacent poles. Another type of machine which is receiving increased attention is the synchronous reluctance motor [3,4] which has also had a long history [5]. In this case the rotor retains saliency but the stator consists of a conventional cylindrical structure. It has been shown that this type of machine competes favorably with the variable reluctance motor when the saliency ratio of the machine reaches 5:1. Machines possessing this degree of saliency and greater have already been reported [6,7].

In the past synchronous reluctance machines were excited with sinusoidal voltages which, in turn, produced sinusoidal currents which produced a spatial MMF with respect to the rotor poles which varied with load. As a result, these machines typically operated at a poor power factor. With the advent of solid state power converters it is now possible to excite the machine not only with sinusoidal waveforms producing an MMF of any desirable spatial position with respect to the rotor poles, but also of current waveforms of any desirable waveshape. In particular, it has been shown that the use of a two phase machine employing unidirectional square waves currents in concentrated windings results in a variable speed drive which utilizes only two transistors in the associated power converter [3].

In a recent paper [4], it was shown that a third harmonic can be added to the fundamental component to help the spatial MMF to a peaked waveform which results in an increased torque per RMS ampere. Unfortunately, the machine employed in [4] was a dual three phase machine having six isolated windings. The associated frequency converter was comprised of six single phase bridges necessitating the use of a minimum of 16 and as many as 24 solid state switching devices depending upon the topology (not discussed in the paper).

Although a three phase, three wire system cannot support a third harmonic component of current, third harmonics can, however, flow in systems having a different number of phases. In particular, five phase systems are particularly attractive since they require the fewest number of transistors beyond a three phase system. The performance of such a five phase reluctance motor excited with an optimized current waveform is the subject of this paper.

Linear Analysis

Figure 1 shows a synchronous reluctance motor with elementary two pole, 5 phase, full pitch, concentrated windings which are 72 degrees displaced in space. The winding function [8] for a typical phase is given in Figure 2. Figure 3 illustrates an idealized representation of the inverse gap function in which the flux is assumed to be only radially directed. The spatial MMF pattern at any instant resulting from the coil currents is determined by the instantaneous currents in all the coils. The rotational movement of the pattern with time is decided by the time variation of these currents; i.e. the current waveforms. Figure 4 shows a five phase inverter which can be used to generate both fundamental and third harmonic current components in the motor windings by means of pulse width modulation. In general, with five phases, the following current waveforms can be assumed,

$$
\begin{aligned}
i_a &= \sqrt{2}\,[I_1 \sin\theta + I_3 \sin 3\theta] \\
i_b &= \sqrt{2}\,[I_1 \sin(\theta - \tfrac{2\pi}{5}) + I_3 \sin 3(\theta - \tfrac{2\pi}{5})] \\
i_c &= \sqrt{2}\,[I_1 \sin(\theta - \tfrac{4\pi}{5}) + I_3 \sin 3(\theta - \tfrac{4\pi}{5})] \\
i_d &= \sqrt{2}\,[I_1 \sin(\theta + \tfrac{4\pi}{5}) + I_3 \sin 3(\theta + \tfrac{4\pi}{5})] \\
i_e &= \sqrt{2}\,[I_1 \sin(\theta + \tfrac{2\pi}{5}) + I_3 \sin 3(\theta + \tfrac{2\pi}{5})]
\end{aligned}
\qquad (1)
$$

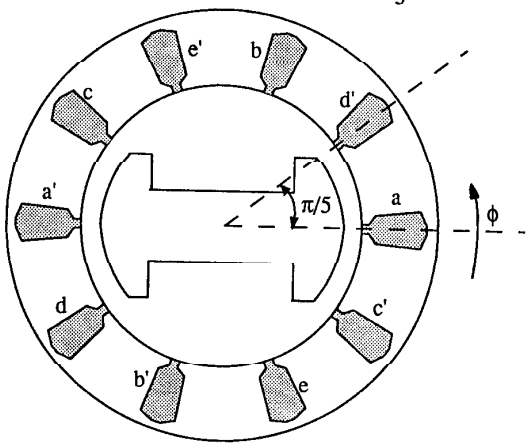

Fig. 1 Synchronous reluctance motor with 2 pole, 5 phase concentrated windings

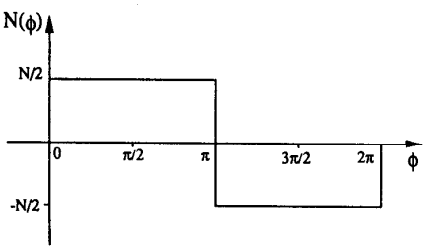

Fig. 2 Winding function for each phase of 5 phase synchronous reluctance machine.

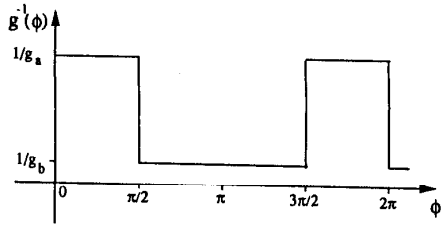

Fig. 3 Air-gap function for a synchronous reluctance machine.

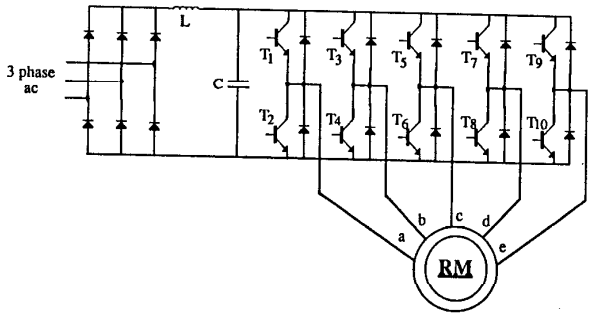

Fig. 4 The 5 phase current regulated pulse width modulation.

The spatial MMF pattern and its fundamental component corresponding to five phase excitation is shown in Figure 5 with $I_3 = 0$. When the windings are excited only with a fundamental and no third harmonic, this type of excitation is termed Type I excitation. Figure 6 shows the spatial MMF and its fundamental if only the third harmonic of the current waveforms is applied. Finally, in Figure 7 the resulting MMF waveform produced by both the fundamental and a typical third harmonic current (Type II excitation). The corresponding current waveform of one phase is shown in Figure 8 . Again, both the exact form of the MMF as well as the combination of the first and third harmonic components are plotted. Note that the peak MMF has been increased which will be later shown to increase the resultant torque per ampere ratio.

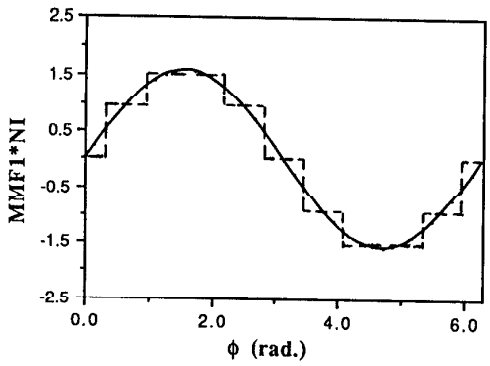

Fig. 5 The spatial MMF pattern and its fundamental if only the fundamental of the current waveform is applied.

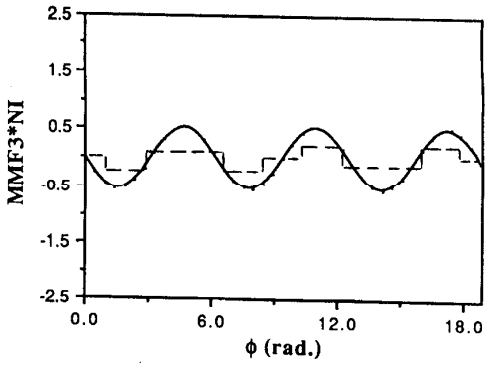

Fig. 6 The spatial MMF and its fundamental if only the third harmonic of the current waveform is applied.

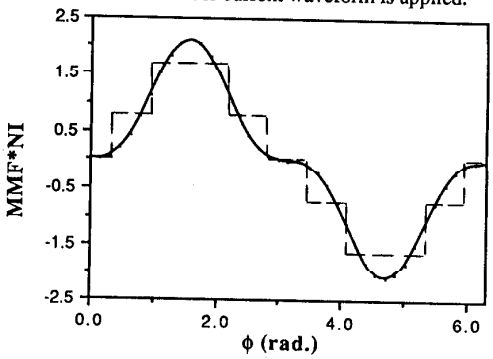

Fig. 7 The resulting MMF waveform produced by both a fundamental and third harmonic current component.

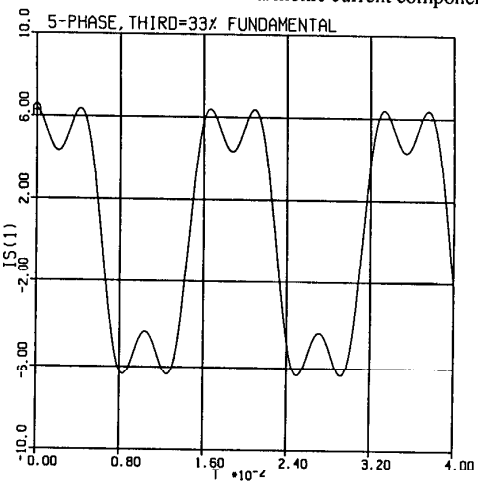

Fig. 8 Input current waveform illustrating an addition of third harmonic of current equal to 33% of the fundamental.

Reluctance Motor Torque Analysis

In this section the air-gap torque of a synchronous reluctance machine containing both first and third spatial harmonics [4,9] is presented. It is assumed that iron is infinitely permeable, and the effect of saturation, tooth harmonics, fringing are neglected. The current loading, which is the effective amperes per meter of periphery, can then be represented by

$$\Delta = \frac{mPN_pIK_pK_d}{\pi D} \qquad (2)$$

where D is the stator inner diameter, N_p is the number of turns per pole per phase, I is the rms current in each phase, K_p and K_d are pitch and distribution factors respectively. Equation (3) gives the peak of the air-gap fundamental MMF wave of a P-pole, m-phase winding:

$$F_1 = \frac{\sqrt{2}\, D\, \Delta_1}{P} \tag{3}$$

Similarly, the peak of air-gap third harmonic MMF wave is given by

$$F_3 = \frac{\sqrt{2}\, D\, \Delta_3}{P} \tag{4}$$

The air-gap flux density is given by

$$B = \frac{4\pi\, 10^{-7}}{g} F \tag{5}$$

where g is the air-gap under the pole. The resultant MMF due to the first and third harmonic is given by

$$F = F_1 \sin\frac{P}{2}\theta - F_3 \sin 3\frac{P}{2}\theta \tag{6}$$

In the ideal case, flux in the air-gap is radial and only exists under the pole arc. Therefore, the ideal energy in the air-gap under the pole, shown in Figure 9, is

$$W = \frac{\pi\, D\, L\, g\, 10^7}{8\,\pi} \frac{1}{\left(\frac{\pi}{P}\right)} \int_{\frac{\pi}{2}-\frac{\tau_p}{2}-\alpha}^{\frac{\pi}{2}+\frac{\tau_p}{2}-\alpha} B^2\, d\theta \tag{7}$$

The derivative of this quantity with respect to α gives the torque

$$T_e = -k\{(\frac{F_1^2}{2} + \frac{F_1 F_3}{3}[\cos(2\alpha+\tau_p) - \cos(-2\alpha+\tau_p)] + \frac{F_3^2}{18}[\cos(6\alpha+3\tau_p) - \cos(-6\alpha+3\tau_p)] + \frac{F_1 F_3}{3}[\cos(4\alpha+2\tau_p) - \cos(-4\alpha+2\tau_p)]\} \tag{8}$$

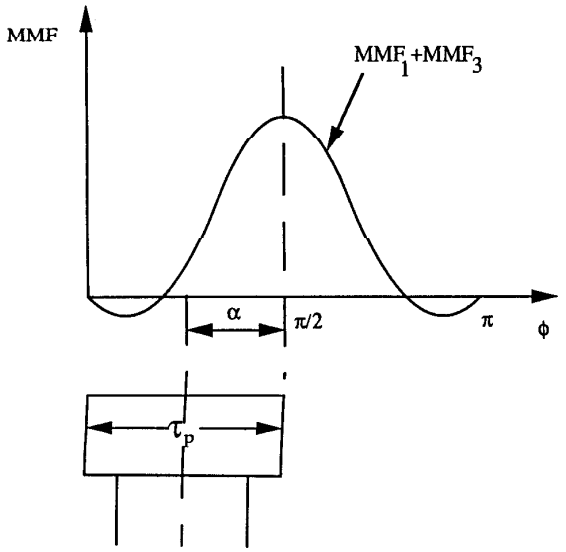

Fig. 9 Air-gap MMF with respect to the pole arc.

It is possible to use Equation (8) to evaluate the effect of the addition of the third harmonic and also the variation of pole arc τ_p as well as current angle α. Using the following minimization criteria

$$\text{Min. } \{-T\}$$
$$\text{s.t.} \quad 0 < \alpha < \frac{\pi}{2}$$
$$0 < \tau_p < \pi$$
$$I_1^2 + I_3^2 = I^2$$

it was determined that a 90 degree pole arc and 45 degree current angle are the optimum values. The optimum amount of third harmonic required was about 33% of the fundamental current. Figure 10 shows the variation of torque with respect to the amount of third harmonic added and also current angle.

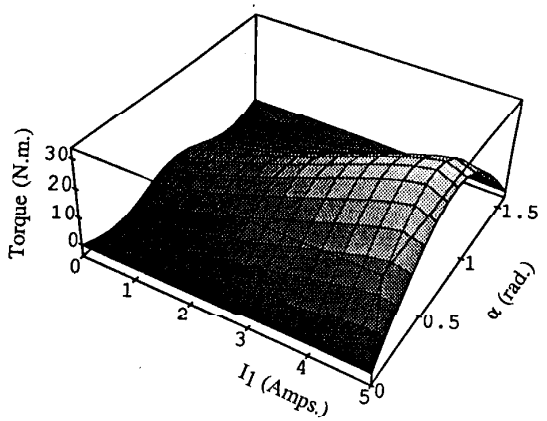

Fig. 10 Variation of torque with current angle and the amount of third harmonic added for 90 degree pole arc.

Winding Function Approach

In this section the winding function approach is used to find the electromagnetic torque and also the input voltages. Again it is assumed that the iron is linear, stator windings are identical with axes of symmetry and that eddy current, friction, and windage losses are neglected.

Stator Voltage Equations

The voltage equations for the stator windings can be written

$$V_S = [R_S] I_S + \frac{d\Lambda_S}{dt} \tag{9}$$

where the vectors V_S, I_S, and Λ_S are defined by

$$\Lambda_S = [L_{SS}]\, I_S \tag{10}$$

and

$$I_S = [i_a^s\ i_b^s\ \ldots\ i_e^s]^t \tag{11}$$

$$V_S = [v_a^s\ v_b^s\ \ldots\ v_e^s]^t \tag{12}$$

and "t" denotes the transpose. The matrix $[R_S]$ is a 5 by 5 matrix given by

$$[R_S] = r_S\, [I] \tag{13}$$

where the matrix [I] is a 5 by 5 identity matrix and r_S is the resistance of each coil assuming all coils are similar.

Due to conservation of energy, the inductance matrix $[L_{SS}]$ is a symmetric 5 by 5 matrix of the form

$$[L_{ss}]=\begin{pmatrix} L^s_{aa} & L^s_{ab} & \cdots & L^s_{ae} \\ L^s_{ba} & L^s_{bb} & \cdots & L^s_{be} \\ \vdots & \vdots & \cdots & \vdots \\ L^s_{ea} & L^s_{eb} & \cdots & L^s_{ee} \end{pmatrix} \quad (14)$$

Since the inductance matrix $[L_{ss}]$ varies with the position of the rotor, the second term of Eq. (9) can be written as

$$\frac{d\Lambda_s}{dt} = [L_{ss}]\frac{dI_s}{dt} + \frac{d[L_{ss}]}{dt} I_s \quad (15)$$

The second term in the above equation can be written using the chain rule as

$$\frac{d[L_{ss}]}{dt} I_s = \frac{d[L_{ss}]}{d\theta_r}\frac{d\theta_r}{dt} I_s \quad (16)$$

Defining equivalent rotor electrical speed as

$$\omega_r = \frac{d\theta_r}{dt} \quad (17)$$

then

$$\frac{d\Lambda_s}{dt} = [L_{ss}]\frac{dI_s}{dt} + \omega_r \frac{d[L_{ss}]}{d\theta_r} I_s \quad (18)$$

Torque Equation

The electrical torque can be found from the magnetic coenergy W_{co}

$$T_e = \left(\frac{\partial W_{co}}{\partial \theta_r}\right) (\text{Is constant}) \quad (19)$$

In a linear magnetic system the coenergy is equal to the stored magnetic energy

$$W_{co} = \frac{1}{2} I_s^t [L_{ss}] I_s \quad (20)$$

From equations (19-20), considering the fact that the self inductance of each coil is constant, results in

$$T_e = \frac{dL_{ab}}{d\theta_r} i_a i_b + \frac{dL_{ac}}{d\theta_r} i_a i_c + \frac{dL_{ad}}{d\theta_r} i_a i_d + \frac{dL_{ae}}{d\theta_r} i_a i_e + \frac{dL_{bc}}{d\theta_r} i_b i_c + \frac{dL_{bd}}{d\theta_r} i_b i_d + \frac{dL_{be}}{d\theta_r} i_b i_e + \frac{dL_{cd}}{d\theta_r} i_c i_d + \frac{dL_{ce}}{d\theta_r} i_c i_e + \frac{dL_{de}}{d\theta_r} i_d i_e \quad (21)$$

The mutual inductance variation using the method presented in [8] is depicted in Figure 11.

In order to demonstrate the potential improvement obtained by injection of a third harmonic current, the above mentioned approach has been used to simulate a 5 phase SRM using the digital computer. The machine is assumed to have 40 stator slots and 8 poles. Figure 12-a portrays the instantaneous electromagnetic torque of the current obtained from simulation when only the fundamental current waveform is applied (Type I excitation). Figure 12-b presents the torque when a third harmonic component equal to 33% of fundamental is added to the current (Type II excitation). It is important to keep in mind that in this study the total rms current in all cases are maintained the same. Figure 13 illustrates the variation of electromagnetic torque with the current angle α (angle of the stator current phasor with respect to the quadrature axis). It can be noted that a 14% increase in torque at α=45 degrees is obtained, compared to the case without third harmonic current.

Non-Linear Analysis

It is clear that the linear model which has been presented has provided needed insight into determining the principles of the torque production in a 5 phase SRM when excited with both fundamental and third harmonic components of current. However, to properly evaluate and compare the design and performance of a 5 phase SRM, more reliable models are required. For this purpose the magnetic field of the machine under study was modelled in a descretized fashion and solved by a finite element method package [10]. The machine has the same specifications as given in the linear case. In order to evaluate the torque capability in terms of rate of coenergy variation with respect to the rotor position, field plots for numerous different rotor positions were obtained.

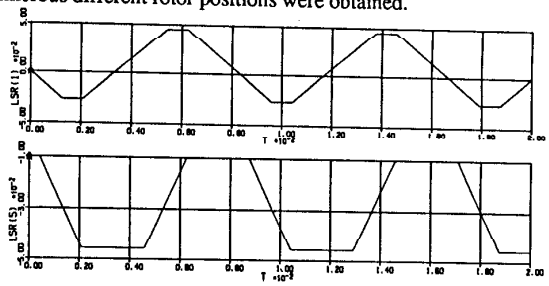

Fig. 11 Variation of mutual inductances with the rotor position.

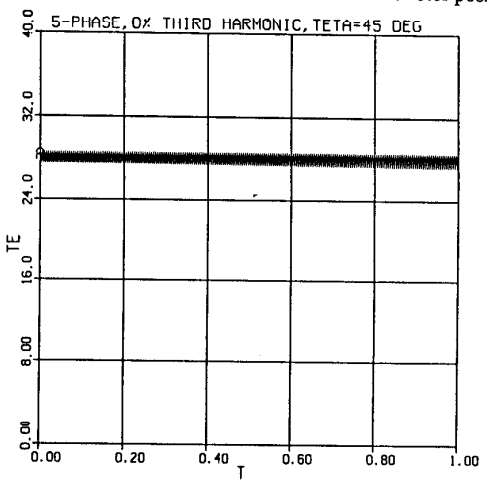

Fig. 12-a Instantaneous electromagnetic torque waveform of 5 phase SRM with only fundamental current waveform applied.

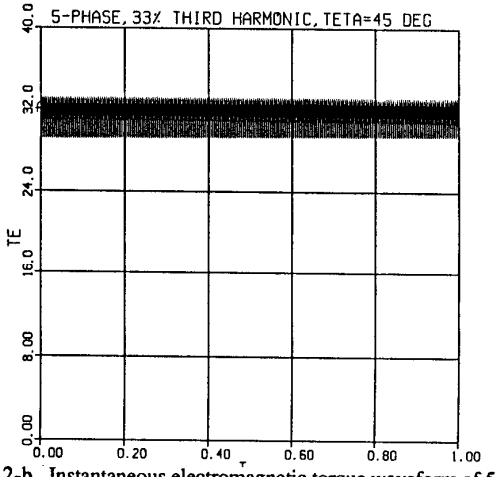

Fig. 12-b Instantaneous electromagnetic torque waveform of 5 phase SRM with addition of 33% third harmonic of current.

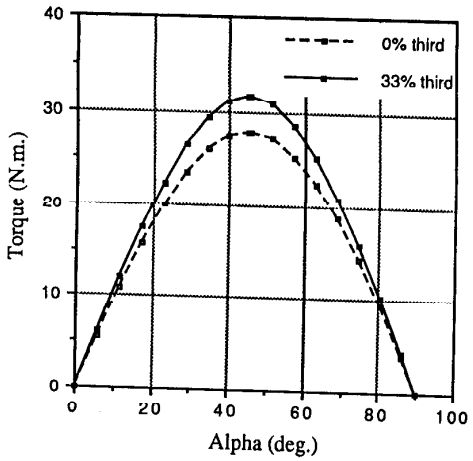

Fig. 13 Torque versus current angle α.

Figures 14 and 15 show vector potential lines (flux lines) for a typical rotor positions for the Type I (no third harmonic) and Type II (fundamental plus third harmonic) SRM's respectively. These plots provide a good descriptive picture of flux distribution. In addition, those points of local saturation can be spotted easily by inspection. It was previously pointed out that the MMF produced by the stator tends to have peaked waveshape in Type II excitation as a result the flux density in the air gap is greater than for Type I excitation. This conclusion is clear from comparison of Figures 16 and 17.

Figures 18 and 19 show the flux density in the stator teeth. Again, because of the peaked MMF waveshape in the air gap, the flux density for the Type II excitation is higher than for the Type I. However, the flux density in the stator core depicted in Figures 20 and 21 show a higher value for Type I than Type II. The reason is that the flux density in the back iron is the integral of flux density in the teeth. This reduced flux density enables the design of deeper slots in the stator and consequently allows for more space for copper in the stator side.

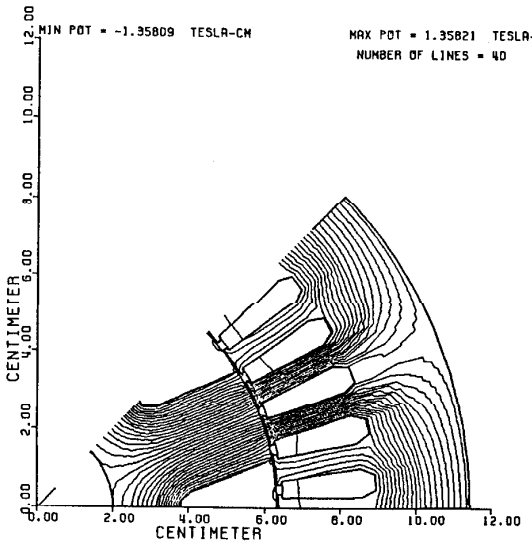

Fig. 14 Vector potential lines for Type I excitation for α=18 degrees.

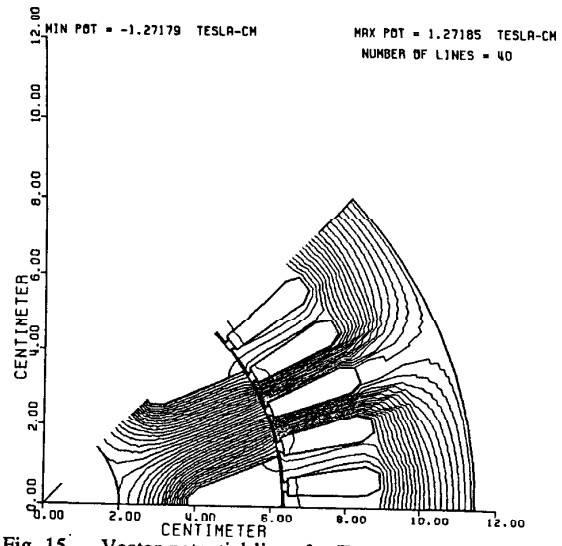

Fig. 15 Vector potential lines for Type II excitation for α=18 degrees.

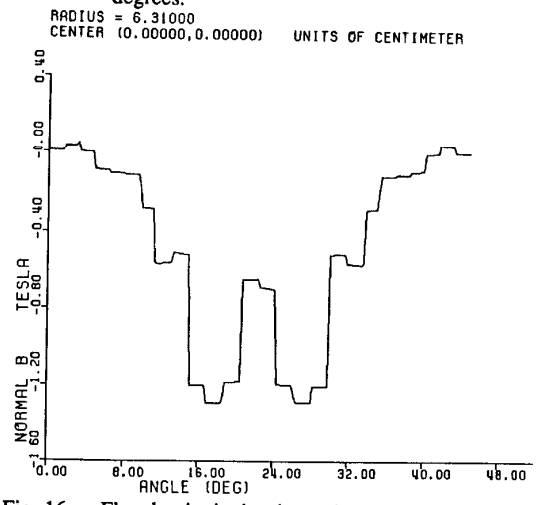

Fig. 16 Flux density in the air gap for Type I excitation for α=18 degrees.

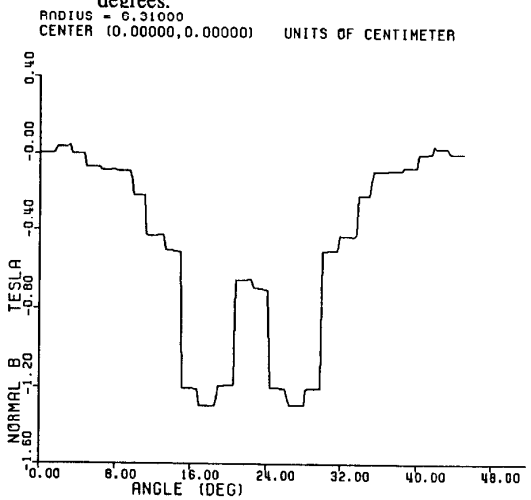

Fig. 17 Flux density in the air gap for Type II excitation for α=18 degrees.

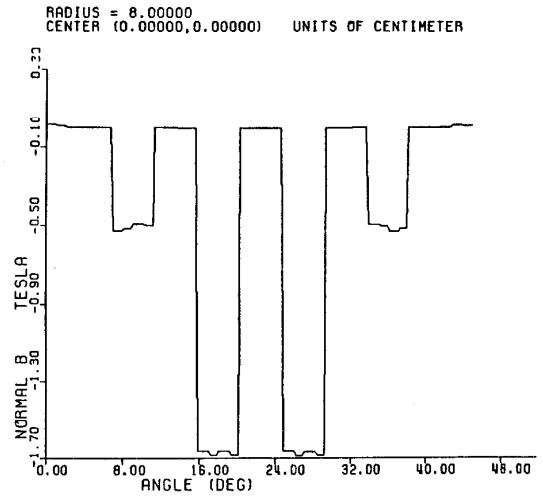

Fig. 18 Flux density in the stator teeth for Type I excitation for α=18 degrees.

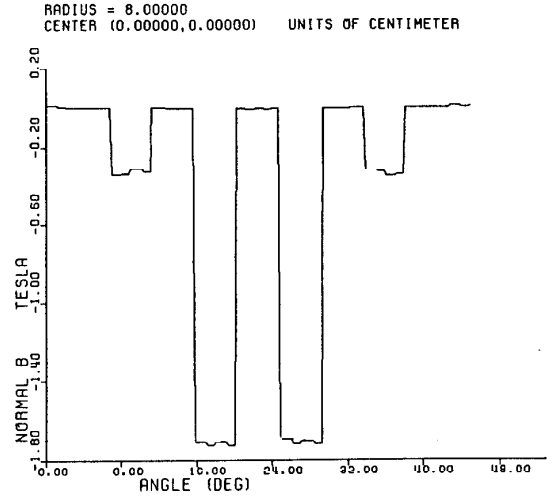

Fig. 19 Flux density in the stator teeth for Type II excitation for α=18 degrees.

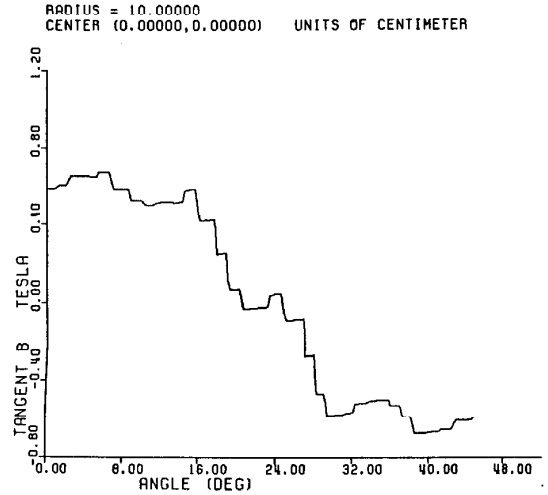

Fig. 20 Flux density in the stator core for Type I excitation for α=18 degrees.

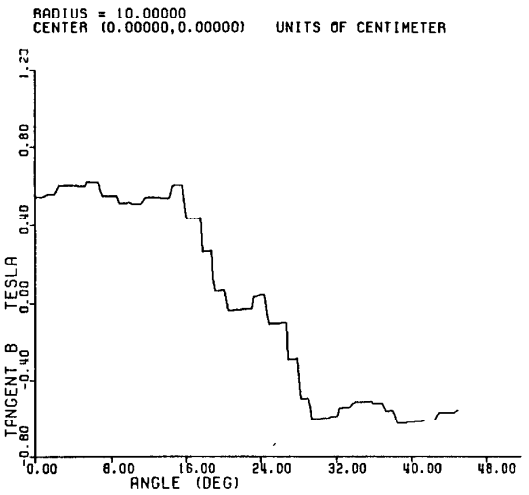

Fig. 21 Flux density in the stator core for Type II excitation for α=18 degrees.

The average torque production is evaluated by calculating the rate of coenergy variation due to the rotor rotation, that is,

$$T_e = -\left(\frac{\Delta W_{co}}{\Delta \theta_{rm}}\right)_{I=\text{const.}} \tag{22}$$

where ΔW_{co} is the coenergy variation corresponding to the variation of rotor angle displacement $\Delta\theta_{rm}$ in mechanical degrees under constant excitation current. Figure 22 illustrates the variation of coenergy with the rotor position. Since the coenergy variations as it is clear are smooth, therefore it is possible to fit them into fifth order polynomials. The derivative of these fifth order polynomials can be used to calculate the electromagnetic toque which are depicted in Figure 23. Note that at least a 10% improvement remains in the developed torque compared to the 14% improvement for the linear case of Figure 13. It is apparent that the saturation of reluctance motors are crucial to the overall performance of such machines.

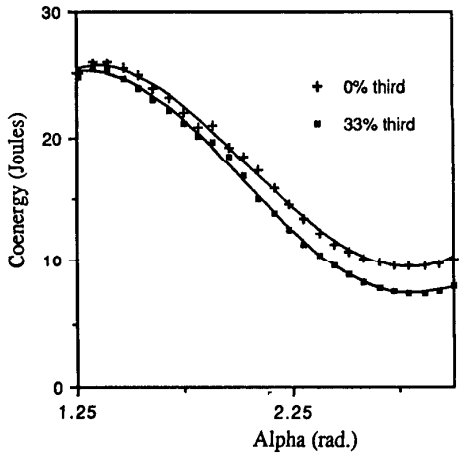

Fig. 22 Variation of coenergy with current angle (α).

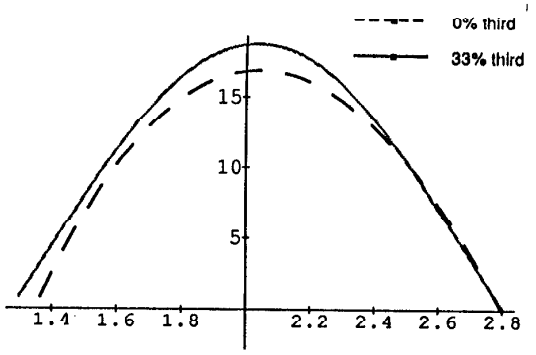

Fig. 23 Variation of electromagnetic torque with current angle (α).

Conclusion

An alternative topology for synchronous reluctance motor is proposed utilizing a five phase current regulated PWM. Linear analysis is used to search for an optimum pole arc and the required third harmonic of current to be added to the fundamental current waveform. These results have been backed by the more detailed analysis using the finite element approach. It was found out that an addition of 33% third harmonic results in 10% more torque even when saturation is properly taken into account. Also, lower flux density in the air gap leaves room for having deeper slots and consequently more copper resulting in a potential further improvement in future designs.

It has been shown that the addition of third harmonic components can be achieved by use of a five phase inverter. It should be mentioned that with proper attention to the physical layout of the phase windings, three phase concentrated winding configurations could also be employed. For example, a scheme which uses an extra inverter leg to force the current in the neutral to form a third harmonic is shown in Figure 24. Alternatively, the neutral can be fed back to a center tap on the dc bus as shown in Figure 25. Such schemes, however, result in an inadequate number of slots unless the machine has a high pole number. Construction of a practical five phase configuration is underway and will be reported in a future paper.

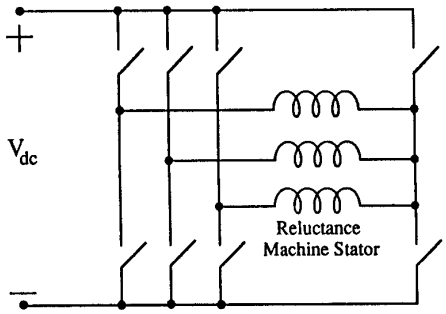

Fig. 24 Three phase, four wire induction machine with neutral current controlled by fourth inverter leg.

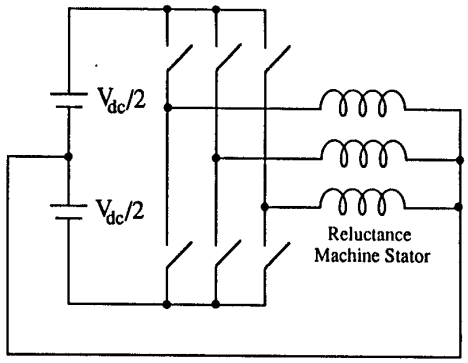

Fig. 25 Three phase, four wire induction machine with neutral current fed back to center tapped DC link.

References

[1] P. J. Lawrenson, J. M. Stephenson, P. T. Blenkinsop, J. Corda, and N. N. Fulton, "Variable-Speed Switched Reluctance Motors," Proceedings IEE, vol. 127, pt. B, no. 4, pp. 253-265, July 1980.

[2] J. Byrne and J.C. Lacy,"Electrodynamic System Comprising a Variable Reluctance Machine" British Patent No. 1321110, 1970, U.S. Patent No. 3,956,678, May 11, 1976.

[3] L. Y. Xu and T. A. Lipo,"Analysis of a Variable Speed Singly-Salient Reluctance Motor Utilizing Only Two Transistor Switches," IEEE Trans. Ind. Appl., vol. 26, no. 2, pp. 229-236, March/April 1990.

[4] J. S. Hsu, S. P. Liou, H.H. Woodson,"Peak-MMF Smooth-Torque Reluctance Motors," IEEE Trans. Energy Conversion, vol. 5, no. 1, pp. 104-109, March 1990.

[5] J. K. Kostko, "Polyphase Reaction Synchronous Motors," American Institute of Electrical Engineers. vol. 45. pp. 1162-1168. Nov. 1923.

[6] S. C. Rao,"Dynamic Performance of Reluctance Motors with Magnetically Anisotropic Rotors," IEEE Trans. Power Apparatus," vol. pas-95,no. 4, pp.1369-1376, July/Aug. 1976.

[7] A. Vagati, "A Reluctance Motor Drive for High Dynamic Performance Applications," in Conf. Rec. 1987 Annual Meeting IEEE Ind. Appl. Soc., pp. 295-302.

[8] T. A. Lipo," Theory and Control of Synchronous Machines," Class Notes, University of Wisconsin-Madison, 1987.

[9] P. L. Alger, The Nature of Induction Machines: Gordon and Breach, New York, 1965.

[10] R. Schiferl, "Design Consideration for Salient Pole Permanent Magnet Synchronous Motors in Variable Speed Drive Applications," Ph.D. Thesis, University of Wisconsin-Madison, 1987